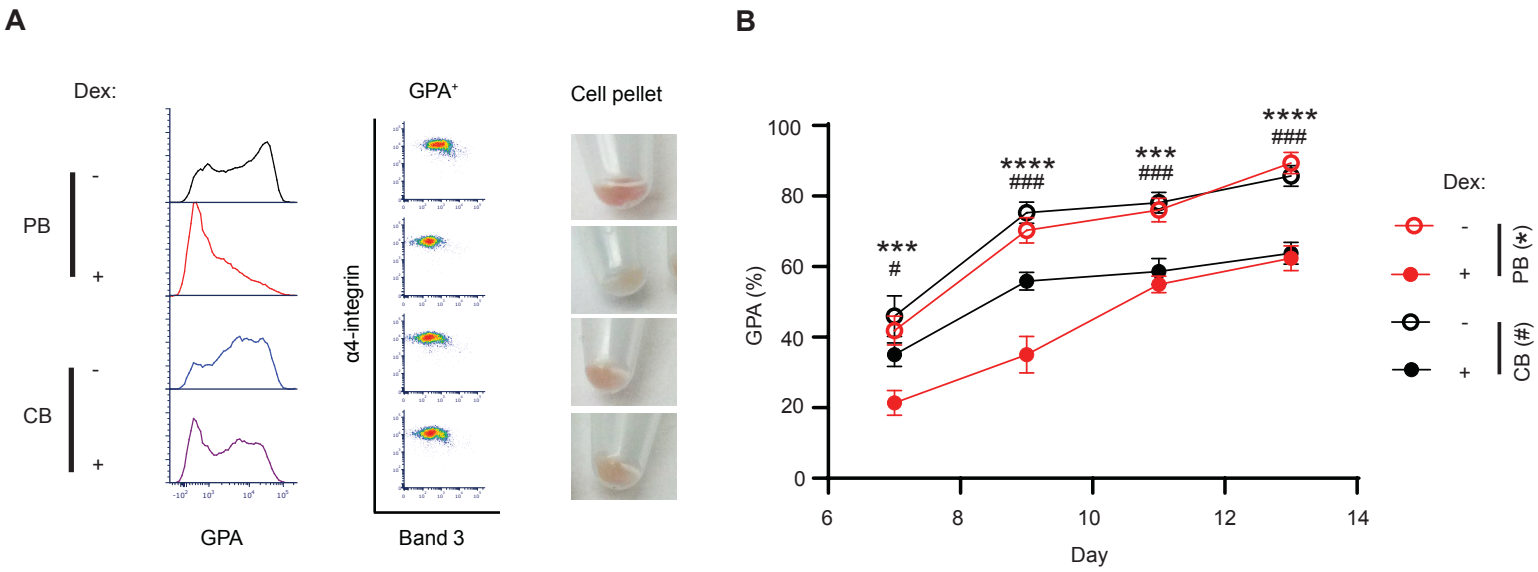

Supplemental Figure 1: Dexamethasone significantly delays Glycophorin A upregulation in terminal erythroblasts in both PB- and CB-derived progenitors.

(A) Representative histograms and cell pellets of PB- and CB-derived progenitors differentiated in the absence (-) or presence (+) of Dex (unsorted day 11). GPA expression as well as Band3 and α4-integrin expression of GPA$^+$ cells are shown. **(B)** Quantification of the percentages of GPA-positive cells following erythroid differentiation of PB- (n=4) and CB-derived (n=4) progenitors in the absence (solid circles) or presence (open circles) of Dex (horizontal lines present means ± SE; $^{*,\#}P < 0.05$, $^{**,\#\#}P < 0.01$, ns-non-significant, by two-way ANOVA with Tukey's post-hoc analysis with corrections for multiple comparisons to assess differences between PB-derived cells (*) and CB-derived cells (#) in the presence or absence of Dex).

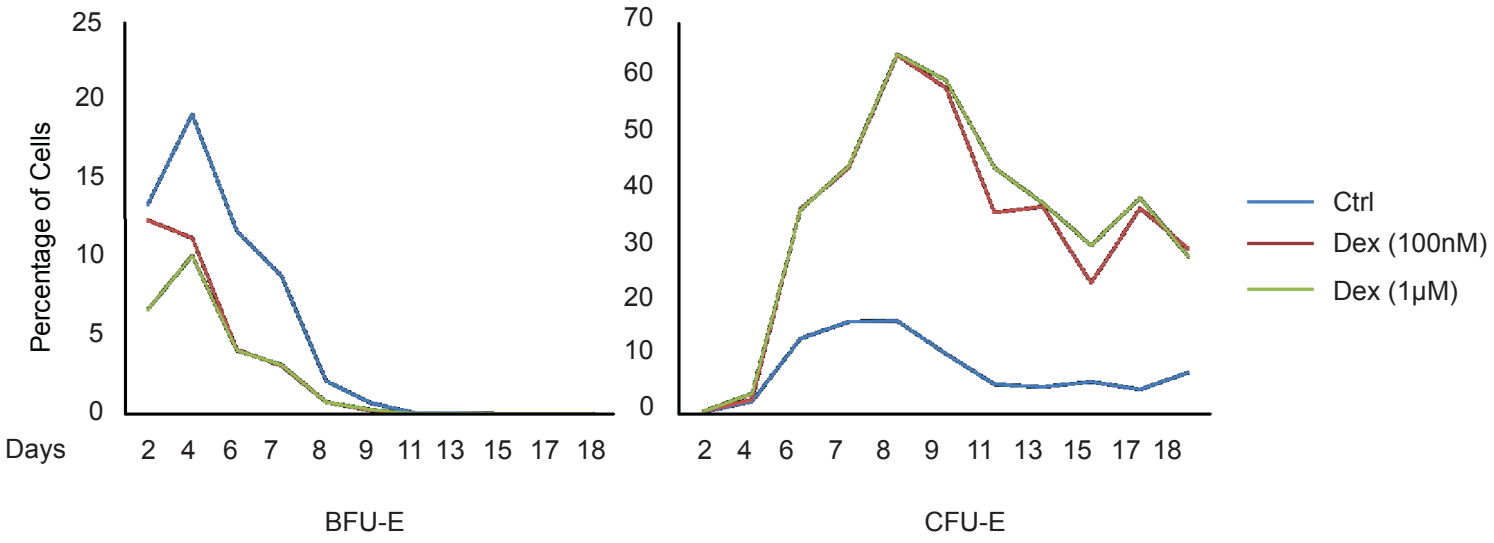

Supplemental Figure 2: Alterations in BFU-E and CFU-E cells as a function of Dexamethasone treatment.

The percentages of BFU-E and CFU-E generated from PB-derived $CD34^+$ progenitors following expansion in the absence (Ctrl) or presence of Dex (100nm and 1μm) are presented.

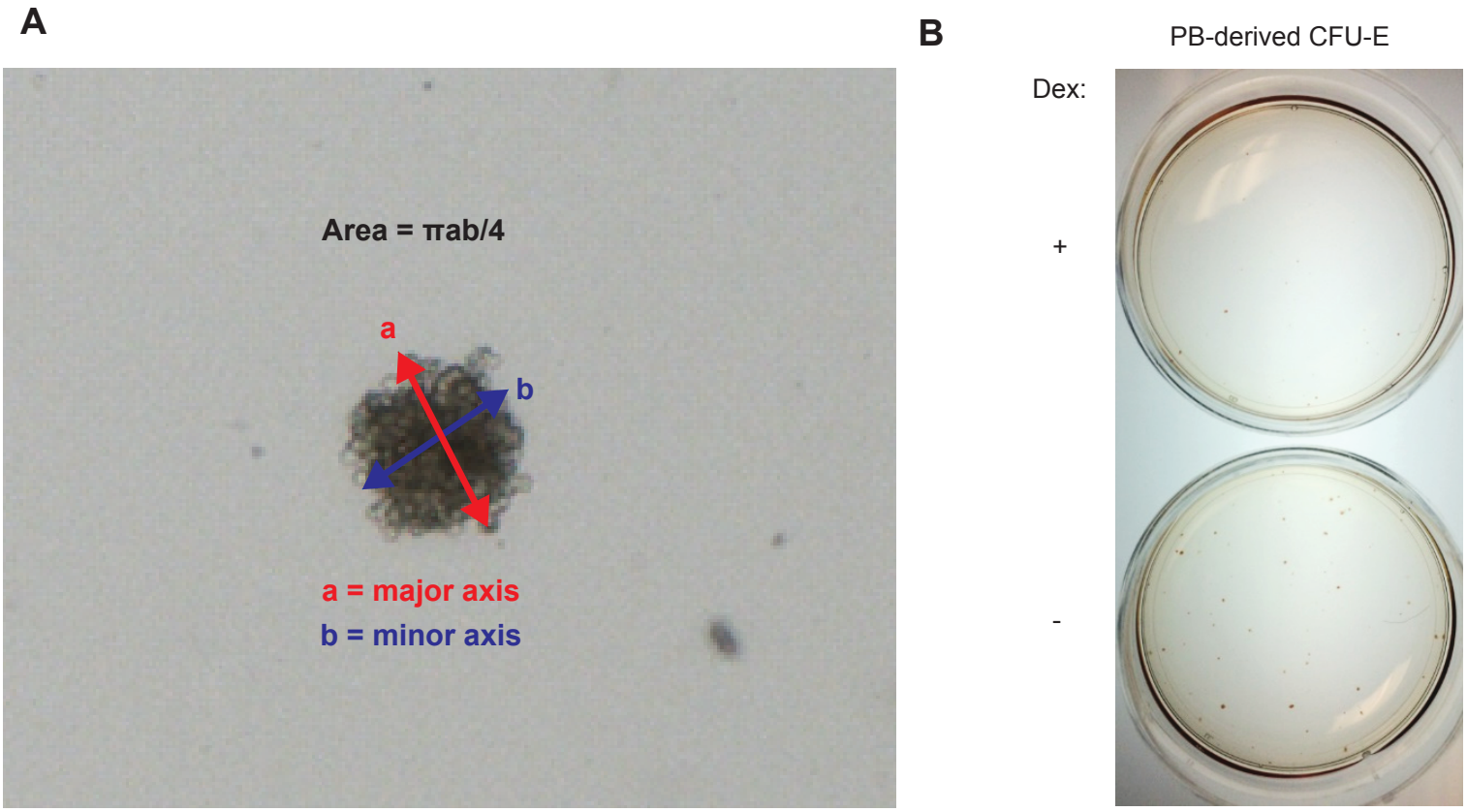

Supplemental Figure 3: Measurement of CFU-E colony area.

(A) Example of a CFU-E colony area measurement. Colony morphology was modeled as an ellipse and the area was determined by measuring the major axis “a” and minor axis “b” to calculate area by the formula A = πab/4. **(B)** Representative images of CFU-E colonies generated from PB-derived CFU-E in the absence (-) or presence (+) of dexamethasone (Dex).

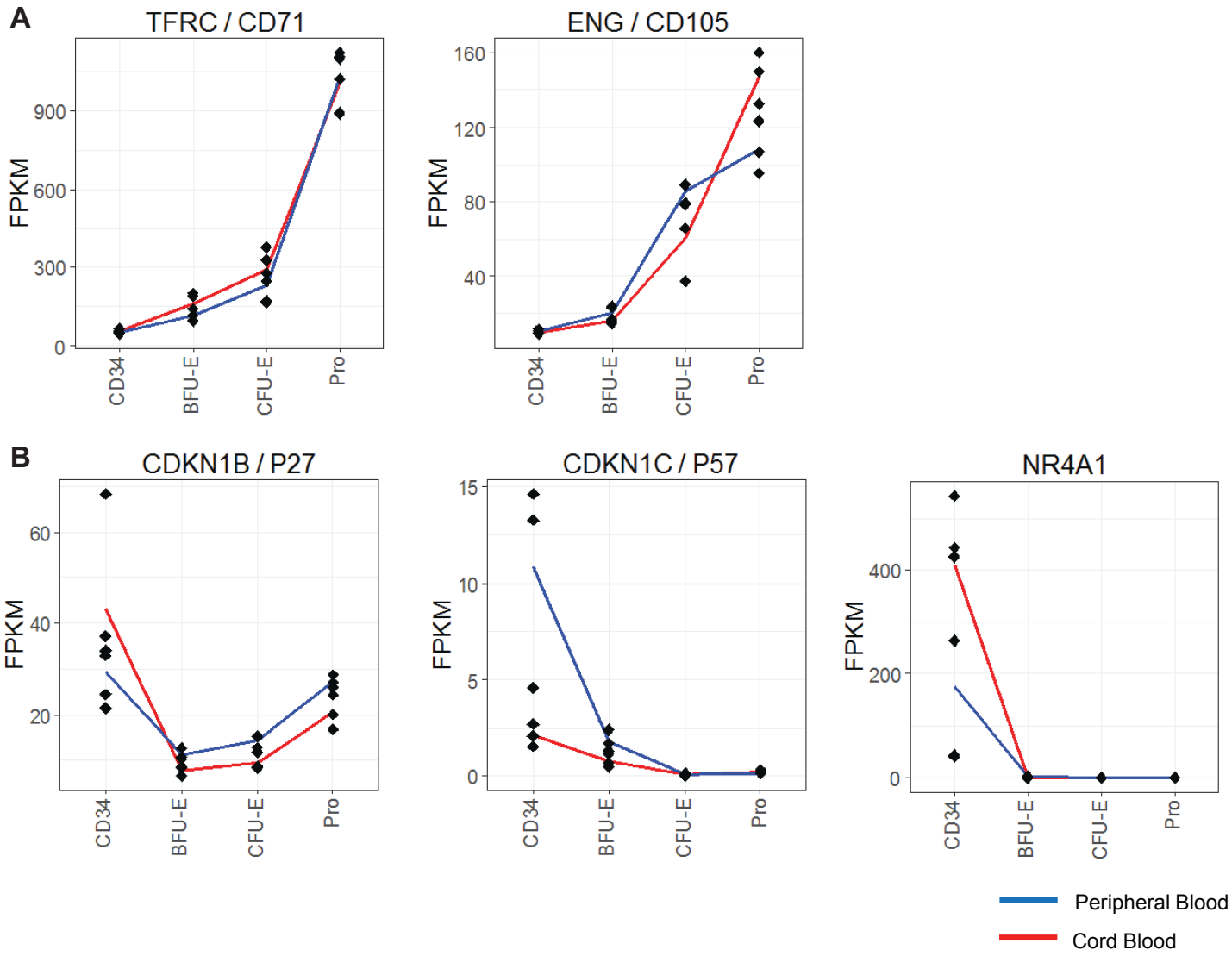

Supplemental Figure 4: Changes in transcripts in PB- and CB-derived progenitors as a function of erythroid differentiation.

Quantification of transcripts of **(A)** *TFRC* (CD71), *ENG* (CD105), and **(B)** *CDKN1B* ($p27^{Kip1}$), *CDKN1C* ($p57^{Kip2}$), and *NR4A1* in sorted erythroid subsets derived from PB (blue) and CB (red) progenitors. Data were originally published in Yan *et al*. 2018 (30).

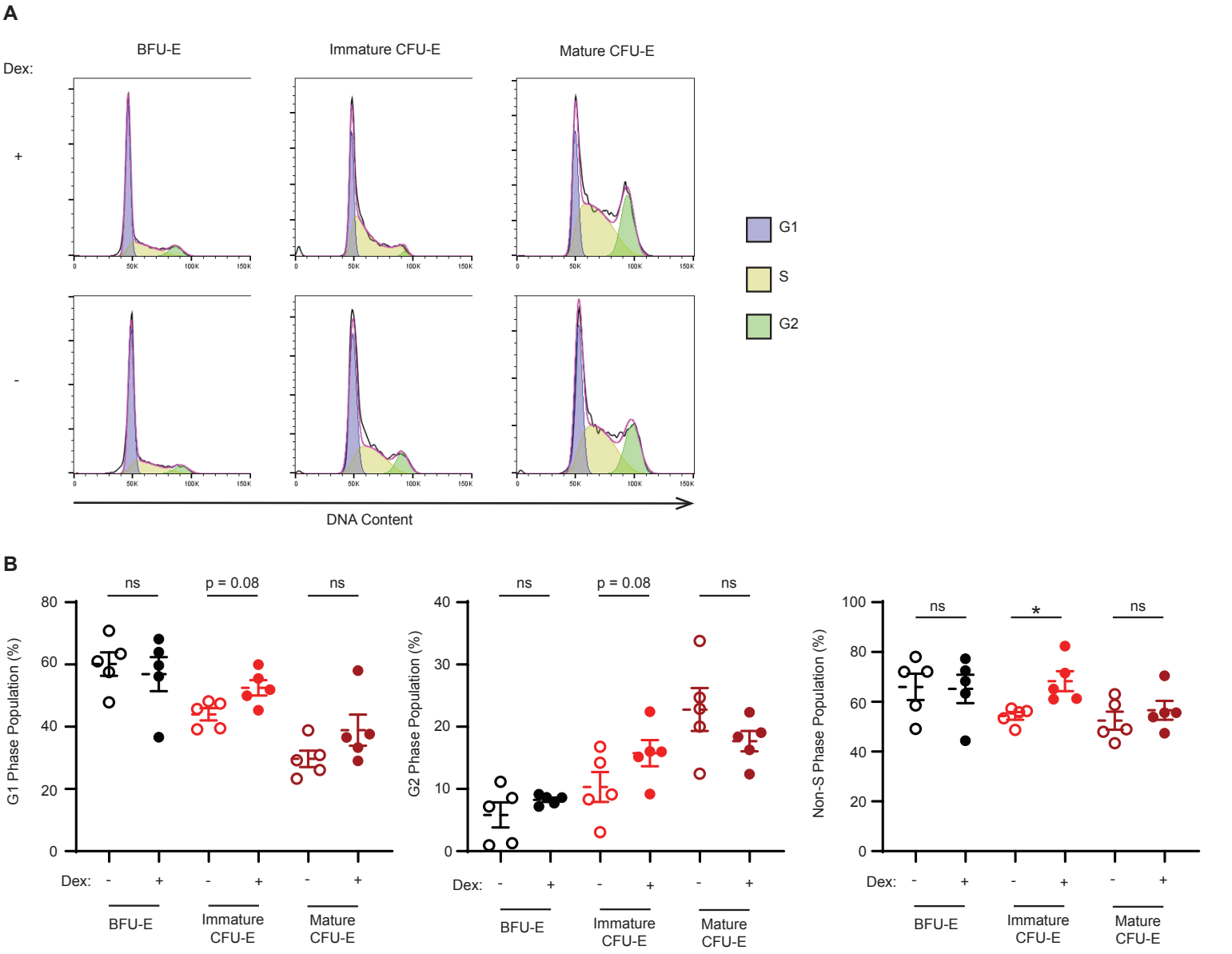

Supplemental Figure 5: Changes in cell cycle dynamics as a function of erythroid differentiation stage and responsiveness to dexamethasone.

(A) Representative cell cycle profiles of PB-derived BFU-E, immature CFU-E and mature CFU-E generated in the absence (-) or presence (+) of dexamethasone. Cells were stained with Hoechst 33342 and evaluated by flow cytometry. The G0/G1, S and G2/M phases of the cell cycle are shown in purple, yellow and green, respectively. **(B)** Quantification of the percentages of cells in G0/G1, G2/M phases and non-S phases populations of the cell cycle within PB-derived BFU-E, immature CFU-E and mature CFU-E subsets in the absence (-) or presence (+) of dexamethasone (n = 5). Means ± SE are shown; ns, non-significant, *$P < 0.05$, by 2-tailed Student's *t* test.

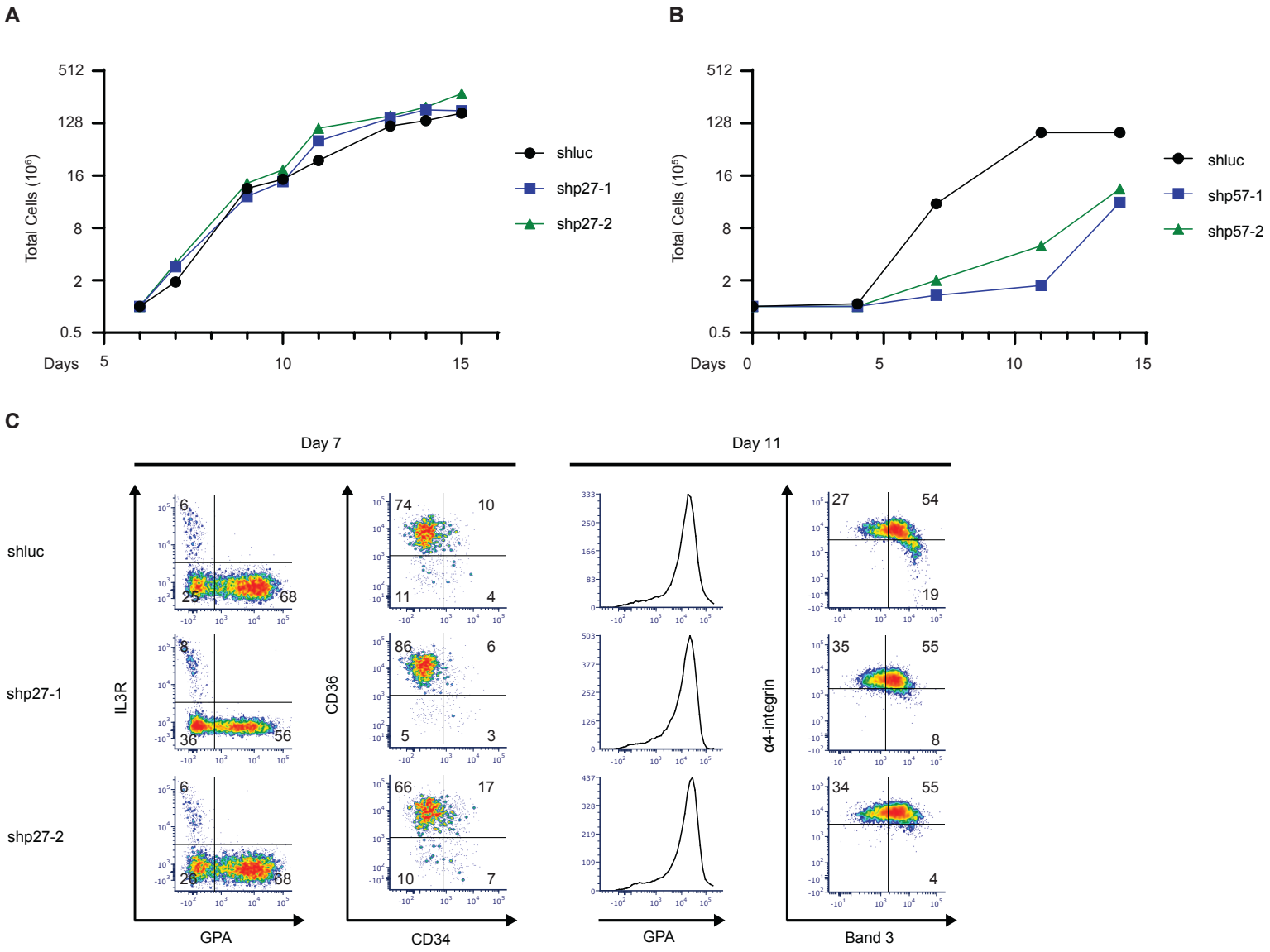

Supplemental Figure 6: Impact of $p57^{Kip2}$ and $p27^{Kip1}$ downregulation on the growth and differentiation of PB $CD34^+$ progenitors

(A) PB-derived $CD34^+$ progenitors were transduced with lentiviral vectors harboring an shRNA targeting a control gene (luciferase) or $p27^{Kip1}$ (two different shRNAs, labelled 1 and 2, are shown). The expansion of these progenitors between days 6 and 15 are presented (results represent data from 1 of 3 independent experiments). **(B)** PB-derived $CD34^+$ progenitors were transduced with lentiviral vectors harboring an shRNA targeting a control gene (luciferase) or $p57^{Kip2}$ (two different shRNAs, labelled 1 and 2, are shown). The expansion of these progenitors between days 0 and 15 are shown. **(C)** Flow cytograms of PB $CD34^+$ cells transduced with lentivirus for shRNA knockdown of $p27^{Kip1}$ and luciferase control.

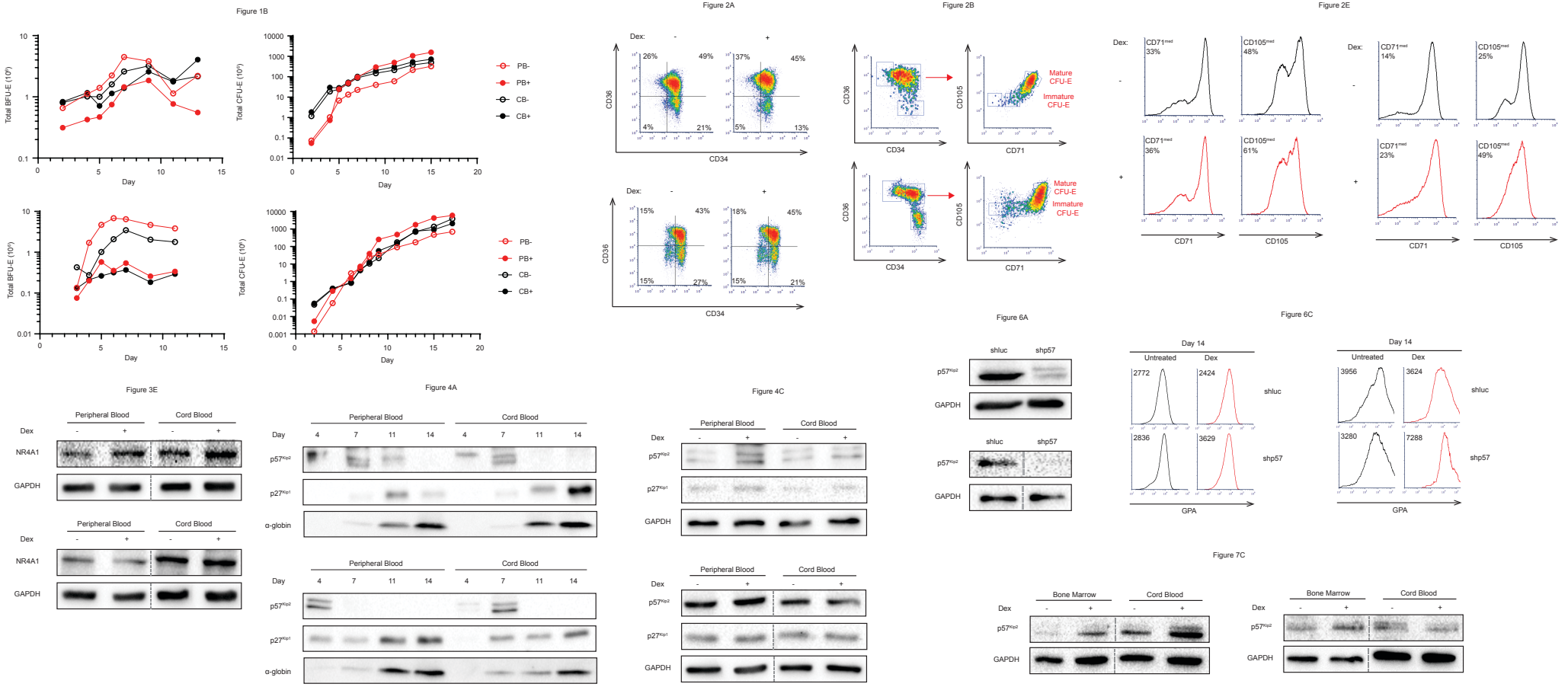

Supplemental Figure 7: Additional representative data related to the main figures.

Figure legends are identical to those in original main related figures.